

## ABSTRACT

SINGH, PALLAVI. Competitive Binding Studies of Substrates and Inhibitors in a Multifunctional Protein - Dehaloperoxidase. (Under the direction of Dr. Stefan Franzen).

Dehaloperoxidase (DHP) is a multifunctional protein. The functions include oxygen transport and enzymatic catalysis. It was first isolated from the terebellid polychaete *Amphitrite ornata*. This worm is found in benthic ecosystems. In the benthic environment, numerous organisms secrete toxic compounds such as halophenols as repellants, i.e. for protection against predators. Dehalperoxidase is an enzyme that oxidizes these toxic halophenols and converts them to less harmful compounds. Since 1996 DHP has been known to function as both a globin and a peroxidase. Recently, two new functions of DHP were discovered as a peroxygenase and an oxidase. These multiple functions depend on the binding sites for substrates and inhibitors, as well as structural factors in the protein such as the distal histidine confirmation and the heme iron oxidation state. These features of DHP are required if one is to comprehend the mechanism of DHP in the presence of different ligands and different substrates/inhibitors. One of the great challenges of DHP is to understand the switching of functions within same enzyme. One hypothesis is that the substrates themselves trigger competitive binding. Therefore, a competitive binding study of substrates/inhibitors was performed in the presence of the ligands fluoride and azide, which both bind to ferric iron. It was observed that fluoride has weaker binding affinity than azide. Comparison of competitive binding with fluoride and azide binding suggested that the steric effect plays a dominant role.

© Copyright 2017 Pallavi Singh

All Rights Reserved

Competitive Binding Studies of Substrates and Inhibitors in Dehaloperoxidase

by  
Pallavi Singh

A thesis submitted to the Graduate Faculty of  
North Carolina State University  
in partial fulfillment of the  
requirements for the degree of  
Master of Science

Chemistry

Raleigh, North Carolina  
2017

APPROVED BY:

---

Stefan Franzen  
Committee Chair

---

Tatyana Smirnova

---

Elena Jakubikova

---

Walter Weare

## **DEDICATION**

I dedicate this thesis to my husband, parents, family members and my mentor.

Without their love, support and guidance it was not possible.

## **BIOGRAPHY**

Pallavi Singh was born on 21<sup>st</sup> July, 1990 in India. She completed her high school from Ram Sewak Yadav Smarak Inter College in 2007. She further continued her undergraduate degree in Chemical Engineering from Maulana Azad National Institute of Technology, Bhopal, India. During the four-year degree program, she was fascinated by the Chemistry and decided to pursue higher education. Finally, she pursued her Master's degree in Chemistry under the guidance of Dr. Stefan Franzen. During this journey, she learned about several spectroscopic and analytical techniques as a part of her research. In addition to support her experimental work theoretically she also learned about Computational Chemistry, programming. As she loves to learn new things, she also learned about several statistical tools and process improvement techniques.

## ACKNOWLEDGMENTS

I would like to express my gratitude to my academic advisor Dr. Stefan Franzen. He provided me a productive environment to work and taught me how to face the real world. He has not only supported me in my research but also in personal life. Stefan is friendly and logical in his life's perspective. He is a pragmatic personality. Without his support and guidance, it was not possible for me to complete Master's program.

I would also like to thank Reza Ghiladi. He had been very helpful for suggesting the new ideas for my research. He was always there to help me in the absence of my advisor. I appreciate his help throughout my journey.

Additionally, I would like to thank my colleagues Jing Zhao, Hniang Khamh, Nikolette McCombs and Leiah Carey. My friend, Melanie Chestnut motivated and guided me during hard times. All of them provided the great environment of friendliness and happiness which supported a lot during my degree.

Finally, I would like to appreciate the actions of my soul mate, Arun Kumar. He believed in my capabilities and supported me in every phase of life.

## TABLE OF CONTENTS

<b>LIST OF TABLES .....</b>	<b>VII</b>
<b>LIST OF FIGURES .....</b>	<b>VIII</b>
<b>CHAPTER 1 .....</b>	<b>1</b>
1.0 INTRODUCTION.....	2
1.1 HEME PROTEINS & DEHALOPEROXIDASE.....	2
1.1.1 Hemoglobin.....	9
1.1.2 Horse Heart Myoglobin .....	9
1.1.3 Horse Radish Peroxidase .....	10
1.1.4 CHLOROPEROXIDASE.....	10
1.2 FTIR in Hemeproteins .....	11
1.3 Justification for study of azide adducts of DHP .....	12
<b>CHAPTER 2 .....</b>	<b>14</b>
2.0 MATERIALS AND METHODS / SPECTROMETERS .....	15
2.1 SPECTROMETERS .....	15
2.1.1 Infrared Spectrometer .....	15
2.2 EXPERIMENT .....	16
2.2.1 Azide and Fluoride Assays (UV-Vis).....	17
2.2.2 Infrared Spectroscopy of Heme Azide Adducts .....	20
2.3 DENSITY FUNCTIONAL THEORY CALCULATIONS .....	21

<b>CHAPTER 3</b> .....	<b>23</b>
3.0 RESULTS .....	24
3.1 AZIDE BINDING STUDIES.....	24
3.2 INFRARED SPECTROSCOPY .....	28
3.3 DENSITY FUNCTIONAL THEORY .....	29
<b>CHAPTER 4</b> .....	<b>32</b>
4.0 DISCUSSION .....	33
4.1 UV-VIS SPECTROSCOPY.....	34
4.2 FTIR .....	36
4.3 DFT CALCULATIONS.....	37
<b>CHAPTER 5</b> .....	<b>38</b>
5.0 CONCLUSION .....	39
<b>REFERENCES</b> .....	<b>40</b>
<b>APPENDIX</b> .....	<b>48</b>
S1. BANDS OF AZIDE DHP IN THE PRESENCE OF SUBSTRATES/INHIBITORS .....	49
S2. OVERLAPPED CRYSTAL STRUCTURES OF AZIDE AND SUBSTRATES/INHIBITORS.....	50

## LIST OF TABLES

Table 1 FTIR Settings Parameter .....	21
Table 2 Dissociation Constants of azide in WT DHPA & B. Dissociation constants of azide and fluoride in the presence of different substrates and inhibitors in DHPA.....	27
Table 3 Single Point Energies of Azide, Fluoride and its adducts in DHP .....	29
Table 4 Binding Energies of azide and Substrate/inhibitor in Dehaloperoxidase.....	30

## LIST OF FIGURES

Figure 1 <i>Amphitrite ornata</i> .....	2
Figure 2 Open Conformation of Dehaloperoxidase (PDB 3DR9) .....	6
Figure 3 Closed Conformation of Dehaloperoxidase (PDB 2QFK) .....	7
Figure 4 Fourier Transform Infrared Spectrometer .....	16
Figure 5 Hemeazide Complex Model .....	18
Figure 6 Model for binding of azide to heme .....	19
Figure 7 UV-Vis Spectrum of Azide titration of WT DHPA .....	26
Figure 8 Dihedral Angle ( $\angle 123$ ) for azide rotation .....	28
Figure 9 FTIR spectrum a) Blue spectrum: DHP, Azide 2 mM b) Red spectrum: DHP, Azide 2mM and DBP 1 mM c) Black spectrum: DHP, Azide 2mM and DBP 2 mM .....	29
Figure 10 Relative Energy of Rotation .....	31
Figure 11 a) Azide (conformation 2) and 4-bromophenol overlapped crystal structures b) Azide (conformation 2) and trichlorophenol overlapped crystal structures c) overlapped crystal structures of azide (conformation 2) and tribromophenol .....	36
Figure 12 a) Overlapped crystal structures of 2,4,6-TCP, 2,4,6-TBP and Azide (Conformation 2) b) Distances of the closest atoms of 2,4,6-TCP and 2,4,6-TBP from Fe .....	37

# CHAPTER 1

## 1.0 Introduction

### 1.1 Heme Proteins & Dehaloperoxidase

Heme proteins are enzymes responsible for a variety of functions in living creatures. Dehaloperoxidase (DHP), a first hemoglobin discovered that has biologically relevant oxidative functions, such as peroxidase, peroxygenase and oxidase.

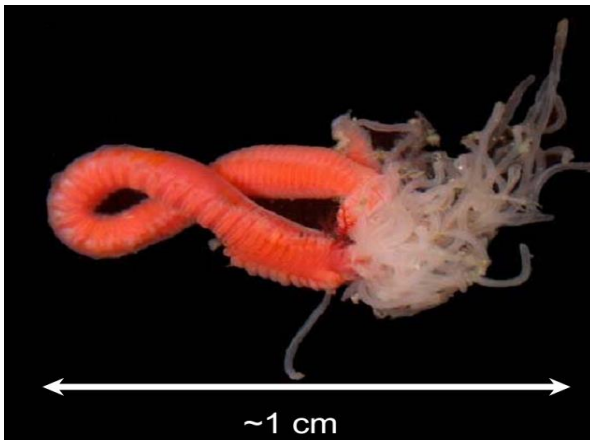


Figure 1 *Amphitrite ornata*

This suggests, DHP is an enzyme that can switch functions, but how does it accomplish this unusual feat? We have advanced the hypothesis that substrate binding itself can cause changes in structure that trigger changes in function. For this reason, new methods to test the strength and structure of bound substrates are needed. Such studies are a major focus of this thesis.

The structural origin of the switching function has become a major focus for current research. Phylogenetic comparison of the amino acid sequence combined with the structural data showing a globin fold strongly suggest that DHP evolved from an ancient oxygen carrier<sup>1</sup>.

When it functions as hemoglobin, O<sub>2</sub> binds to DHP reversibly (Fe<sup>2+</sup>). Similarly, hemoglobin also mainly bind to oxygen reversibly but other heme proteins such as peroxidase, oxidase, peroxygenase are responsible for irreversible enzymatic oxidations.

DHP belongs to the globin<sup>2,3</sup> family<sup>4</sup> which has similar characteristics such as hemoglobin and myoglobin . This multifunctional<sup>5</sup> enzyme was first isolated from a terebellid polychaete found in benthic ecosystem known as *Amphitrite ornata* (Figure 1). It co-inhabits with the other species such as *Notomatus lobatus* which secrete toxic phenols<sup>6</sup>. *Amphitrite ornata* oxidizes these toxic halophenols and converts them into dihaloquinones. The native substrate of the peroxidase function has been thought to be 2,4,6-tribromophenol<sup>7</sup>. In 2010, it was realized that 4-bromophenol is an inhibitor of the peroxidase mechanism<sup>7</sup>. The fact that new functions were discovered more recently indicates that DHP has other substrates, which may include 5-bromoindole and 2,4-dibromophenol among others<sup>8</sup>.

To understand the switching of functions in DHP, it is important to develop the study its structure. DHP has 3/3  $\alpha$ -helical protein structure which is common to globins. It's structure is similar to many myoglobins with eight  $\alpha$ -helices and 3/3  $\alpha$ -helical folds<sup>9</sup>. Myoglobin has 8  $\alpha$  helices which contributes to almost 75% of its structure. In myoglobin,  $\alpha$  helices are terminated by proline residues. As DHP has smaller number of amino acids, it is truncated and has fewer terminal amino acids than most myoglobins. It has 137 amino acids but myoglobin has 153 amino acids. The crystal structure of dehaloperoxidase protein in all of its forms is reported to be a dimer in the unit cell. The interfacial area of the contact region for the two halves of the dimer is found to be relatively smaller in comparison to other dimeric proteins, but there are other indications that DHP is a dimeric protein, at least transiently in solution.

Small angle x-ray scattering measurements suggest that that DHP exists 80-90% in the monomer (15.5 kDa) form in solution<sup>9</sup>. This interesting result suggests that DHP is 10-20% dimerized in solution. The importance of this observation is still not known, but it may be related to function.

DHP has two isoforms<sup>10</sup> A and B with 137<sup>11</sup> amino acids each but these isoforms differ by five amino acids ((I9L, R32K, Y34N, N81S, and S91G). Between the two isoforms, DHPB is found to be less stable<sup>12</sup> than DHPA. However, by contrast the catalytic<sup>13</sup> efficiency<sup>14</sup> of DHPB<sup>15,16,17</sup> is three times greater than DHPA. Chemical and thermal denaturation was used to investigate the stability of these isoforms. Denaturation of protein induced by guanidinium<sup>18</sup> hydrochloride and urea was observed at  $1.15 \pm 0.01$  M DHPA and  $1.09 \pm 0.02$  M DHPB, respectively. However, the binding affinity of the heme was reported to be smaller in both the isoforms of DHP than horse skeleton muscle myoglobin.

The previous studies suggested the catalytic efficiency of an enzyme is also effected by the electrostatic charge on the protein. It was observed that increasing the positive charge on DHPA resulted in a greater catalytic efficiency than wild type DHPA. Positive charges can be increased by surface mutations on DHP. These electrostatic charges also effect the interaction of DHP and 2,4,6-TCP substrate<sup>19</sup>. The effect can be explained quite simply by the electrostatic attraction of the negative charge of the phenoxyl anion form of 2,4,6-TCP above the pKa of 6.2 for the positive charges on the protein surface. By increasing the positive charge on the protein surface the attraction for the substrate increases, which could lead to a more rapid diffusion in solution. These electrostatic effects on the binding of 2,4,6-TCP further confirmed by carrying out kinetic assays at varying ionic strength.

To understand the binding of 2,4,6-TCP first we need to focus on the multiple functions of DHP. The globin function of dehaloperoxidase is represented by the reversible binding of oxygen. Oxygen can bind with oxyferrous form of the heme iron in dehaloperoxidase. DHP also functions as a peroxidase<sup>20,21,22,23</sup>. Its activity ( $\text{Fe}^{3+}$ )<sup>24</sup> is catalyzed<sup>25</sup> in the presence of  $\text{H}_2\text{O}_2$ . Peroxidase<sup>26</sup> ( $\text{Fe}^{2+}$ ) oxidizes<sup>27</sup> the toxic phenols<sup>28</sup> such as 2,4,6 tribromophenol to the corresponding 2,6 dihaloquinone<sup>29,30,31,32,33</sup>. Peroxidase function is activated in the presence of  $\text{H}_2\text{O}_2$ .

Recently, peroxygenase and oxidase functions were discovered in DHP. Those studies confirmed that indoles are substrates for these functions<sup>26</sup>. The peroxygenase function requires indoles to bind in the distal pocket<sup>34,35</sup>. It leads DHP to 5cHS conformation and forces distal histidine to exposed to solvent. It is similar what was observed in the presence of monohalophenol binding<sup>36</sup>. DHP is unique among the hemoglobins in that it has a large distal pocket. The distal pocket is internal space above the heme. In most globins, the distal pocket is quite small and it can only support the binding of diatomic ligands<sup>37,38</sup> to the heme iron. In DHP, substrates do not bind to the heme iron, however, they bind internally. The simplest model suggest that substrate binding might play an important role in function switching among the four functions known in DHP.

The distal histidine in DHP is Histidine 55 ( $\text{His}^{55}$ ). It has two main conformations<sup>39</sup> known as open and closed<sup>40</sup>. The closed<sup>41,42,28</sup> conformation (PDB 1EW6) consists of an interaction of heme bound water or ligand with the histidine<sup>43</sup> via hydrogen bonding<sup>44</sup>. Hydrogen bonding in the oxyferrous of DHP<sup>24</sup> involves interaction of the N-H of  $\text{His}^{55}$  with bound oxygen. In the metaquo form, the hydrogen bonding involves an interaction of the O-H

of water with the nitrogen of His<sup>55</sup>. In both six-coordinate forms the histidine is observed in the distal pocket pointing towards the heme ligand. However, the five coordinate heme does not have an interaction with His<sup>55</sup> and therefore the histidine is observed in a solvent-exposed conformation interacting with the heme propionates. This conformation is known as the open conformation.

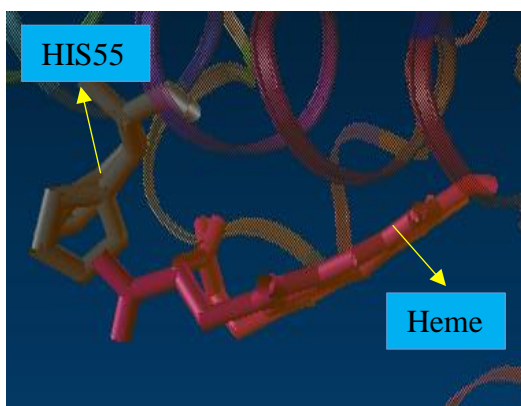


Figure 2 Open Conformation of Dehaloperoxidase (PDB 3DR9)

The open conformation is also observed when 4-halophenol<sup>45</sup> binds in the distal pocket and pushes the distal histidine into the solvent-exposed conformation<sup>46</sup>. In each of these the distal histidine is observed in the open conformation (PDB 3LB2). Although we have structural data there is a need for quantitative data on the binding affinity of these various molecules in the distal pocket of DHP. This quantitative information on internal binding of the substrates/inhibitors can give us a better understanding of DHP function switching.

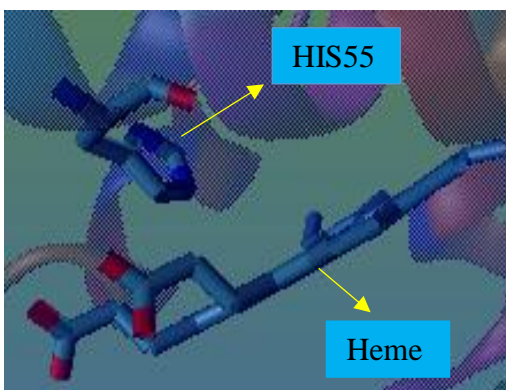


Figure 3 Closed Conformation of Dehaloperoxidase (PDB 2QFK)

From the crystal structures of DHP, histidine was found to be in the closed conformation if heme iron is 6-coordinated. However, crystal structure of DHPCO (6-coordinated) reported the open conformation of histidine. The large population of distal histidine in open conformation at pH 6.0 in DHPCO crystal suggest the structural difference of DHP with other heme other globin proteins, which exhibit the solvent exposed conformation (open or external conformation) at  $\text{pH} < 4.5^{45}$ . It rules out the hypothesis that Fe-ligand determines the conformation of distal histidine or perhaps suggests that the extremely weak hydrogen bonding between CO and His<sup>55</sup> is responsible for the structure. It is known that the hydrogen bonding between CO and His<sup>55</sup> is extremely weak. The solvent exposed conformation shows the interaction of distal histidine with the propionate chains at the distance of 3.82 and 2.73 Angstroms.

DHP has at least two internal binding sites. These can be classified as  $\alpha$  and  $\beta$  binding sites. At  $\alpha$ -site, 2,4,6 tribromophenol and 2,4,6 trichlorophenol bind. This binding site is called substrate binding site. However, 4-bromophenol binds at  $\beta$  site. The binding of 4-bromophenol in the distal pocket reduces the catalytic activity of DHP.

The mechanism for 4-BP binding which results in reduced catalytic activity of DHP, has been investigated using Michealis-Menten and transient-state kinetic analysis<sup>47</sup>. Two new products have been observed during the reaction. Instead of forming compound ES, an inhibitor bound intermediate that possessed blue shifted soret band with two Q band peaks. It was finally recognized as different species from compound RH which is formed in uninhibited enzyme<sup>48</sup>.

Experiments showed that hydroquinone was found to be compete with the oxidation of the native substrate 2,4,6-TBP in the presence of H<sub>2</sub>O<sub>2</sub>. Catalytic oxidation of hydroquinone is so much faster than oxidation of the native substrate that there is no obvious change in the spectrum at 279 nm (where product is normally observed for 2,4,6-TBP oxidation) until all of the hydroquinone has been used up. This is period is known as the lag phase. During this lag phase, DHP is inactivated as hydroquinone oxidizes to 1,4- bezoquinone while inhibiting the oxidation of 2,4,6 tri-halophenols. However, inhibition of oxidation of these tri-halophenols is different in the presence of 4-BP because the inhibitor competes hydroquinone itself<sup>49</sup>. Once the hydroquinone has all been oxidized DHP can immediately resume normal oxidation of 2,4,6-TBP (provided there is sufficient H<sub>2</sub>O<sub>2</sub> present).

Beyond 2,4,6 tri-halophenols, DHP can oxidize other toxic phenols<sup>50</sup>, indoles and even the pyrroles to less harmful compounds. One of the remaining important question in DHP function is the structure and thermodynamics of substrate binding in the distal pocket above the heme.

### 1.1.1 Hemoglobin

Human hemoglobin is composed of proteins formed by a symmetrical pairing of a dimer of polypeptide chains,  $\alpha$  and  $\beta$  globins into a tetrameric structural and functional unit. The tetramer unit contains a large space in which heme prosthetic group is bound through non-covalent forces<sup>51</sup> in hemoglobin. Whereas the surrounding aqueous solution protect the heme prosthetic group iron. Heme iron is ligated to four nitrogens of pyrrole rings. The fifth coordination of iron is ligated to nitrogen of proximal histidine. The structure of hemoglobin has been explored using x-ray crystallography<sup>52</sup>. The quaternary structure was found to be different for the oxy and de-oxy state of the hemoglobin. DHP is a hemoglobin in the sense that it binds oxygen reversibly in fluids (not in muscle), but DHP is clearly not a tetramer. There are dimeric hemoglobins, such as the well-known *Scapharca* clam hemoglobin<sup>53</sup>. DHP may be a dimer under some conditions and thus there may be some similarity here. However, marine hemoglobins can be monomeric. Despite the fact that human and many mammalian hemoglobins are multimeric, there is no rule that says that a hemoglobin must be a multimer.

### 1.1.2 Horse Heart Myoglobin

Another example of heme protein in the globin family is horse heart myoglobin (hhMb). Horse heart myoglobin has been widely studied. The distal histidine (His64Thr, His64Ile and His64Lys) and surface charged (Val67Arg Lys45Glu Lys45Glu/Lys63Glu) variant were studied for the azide binding affinity. Only Val67Arg variant was found to have lower binding affinity than wild type protein. However, the temperature variation<sup>54</sup> for all variant studies

showed the existence of the high and low spin equilibrium. This spectrum is important as a background for the infrared studies of azide binding presented in this thesis.

### **1.1.3 Horse Radish Peroxidase**

Peroxidases have the capability to catalyze the oxidation of substrates via hydrogen peroxide. Dehaloperoxidase has a similar function which is a common characteristic peroxidase family. Horse radish peroxidase is a heme protein which belongs to peroxidase family. The peroxidase activity results in the oxidization of the inorganic and organic compounds in the presence of co-substrate,  $H_2O_2$ . The isoenzyme<sup>55</sup> of horse radish peroxidase is named as horse radish peroxidase C (HRP C). It has 308 amino acids. Horse radish peroxidase has two metal centers. One contains heme and other contains two calcium atoms. Like hemoglobins, heme iron is attached to a proximal histidine (His 170)<sup>56</sup>. The other histidine is found above heme. This site, known as the distal pocket is unoccupied in the resting state. Horse radish peroxidase heme iron has similar binding<sup>55</sup> affinity towards small molecules such as carbon monoxide, as well as anionic ligands as sperm whale myoglobin. The binding of some of these molecules is stabilized via hydrogen bonding through the distal histidine 42 and the distal arginine 38<sup>55</sup>.

### **1.1.4 Chloroperoxidase**

There are other heme proteins which also can function as a dehaloperoxidase. *Caldariomyces fumago* chloroperoxidase is one of them. This enzyme can catalyze the dehalogenation of 2,4,6-halophenols and p-halophenols in the presence of  $H_2O_2$ <sup>57</sup>. It is a robust

dehaloperoxidase as it can also function as a bioremediation catalyst for aromatic dehalogenation reactions.

DHP has similar catalytic function to horseradish peroxidase which involves a high-valent ferryl heme and two single electron transfers from the aromatic substrate to enzyme. Investigation of bioremediation in DHP has failed because of the distal pocket above heme can accommodate 4-halphenols. Binding of these 4-halphenols into the distal pocket results in reduction of catalytic activity of enzyme which is inhibitor of peroxidase of DHP. As distal pocket is surrounded by several<sup>58</sup> hydrophobic amino acids which play an important role to stabilize internal binding including isoleucine near the edge of heme. Mutants L100T and L100F showed increased peroxidase activity than wild type DHP. It suggests the less binding of 4-BP in DHP. Further, the crystal structure of L100F reported the reduced population of 4-BP into the pocket.

## **1.2 FTIR in Hemeproteins**

In order to validate our hypothesis, it is important to establish that the binding of ligand and substrate is mutually exclusive. We used Fourier Transform Infrared (FTIR) spectroscopy tool for validation. Azide can have two spin states low and high spin. There is the equilibrium between low and high spin azide states dehaloperoxidase. Similar equilibrium was observed in horse muscle skeleton myoglobin<sup>54</sup>. Following the similar notion, two bands were also observed in dehaloperoxidase-azide adduct. These two bands resulted corresponding to low and high spin state of azide which exist in equilibrium. By studying the intensity and frequency of this band in the presence of different substrates we were able to address the hypothesis. The

two azide bands were observed corresponding to low and high spin at  $2023\text{ cm}^{-1}$  and  $2046^{54}\text{ cm}^{-1}$ , respectively. The broad band at  $2048\text{ cm}^{-1}$  was assigned corresponding to unbound azide in the protein. A similar study had been also performed with horse heart myoglobin and its mutants without substrates<sup>54</sup>. In that case, the temperature dependent studies showed the increase in the absorption of high spin azide with increase in temperature. However, the intensity of low spin band decreased with temperature.

Typically, it was observed that as the temperature was increased in the presence of azide ion,  $\nu_{\text{max}}$  shifted to the lower energy<sup>54</sup>. However, as the temperature increased, half-band width was also found to be increased. Previous studies showed the ligand bound to heme iron has a narrower bandwidth than free ligands or ligands bound to iron porphyrins in solution. There is also a change in bandwidth<sup>54</sup> as a function of solvent polarity.

Infrared spectroscopy of metal proteins such as hemoglobin or myoglobin suggested the frequency of CO vibration is effected by the electronic configurations, local molecular environment and effective bonding order of carbon monoxide.

### **1.3 Justification for study of azide adducts of DHP**

The characteristics of hemoglobin, myoglobin and peroxidase have been explored but DHP is an enzyme with more than one function. Therefore, it is important to explore how the internal mechanisms work such as monooxygenase, peroxygenase and oxidase functions. There are several factors which accounts for its multiple functions. Flexibility of distal pocket, binding of substrates and inhibitors, binding of ligands, hydrogen bonding interactions, Van der Waals interactions, size of ligands and the binding sites etc. Most of the areas have been

explored but there is still a question how the size of different ligands effect the internal mechanism in the protein or how can we understand the different functions if there is presence of steric effect of ligands.

In order to address the quantitative aspect of binding, competitive<sup>22</sup> binding studies were performed with different substrates/inhibitors in the presence of ligands. Fluoride binds weakly to DHP, however, cyanide binds strongly in DHP. To understand the competitive binding between ligand and substrates, it is important to find a ligand which could have moderate binding in DHP. Therefore, azide was chosen as ligand which is having binding affinity in between fluoride and cyanide.<sup>54</sup>

## CHAPTER 2

## **2.0 Materials and Methods / Spectrometers**

### **2.1 Spectrometers**

#### **2.1.1 Infrared Spectrometer**

The Fourier transform infrared spectrometer is the most important method used to measure the vibrational frequency of normal modes of vibration in molecules. This technique is widely used in heme proteins to observe the peaks of ligand bound to heme iron, e.g. the vibrational frequency of horse heart myoglobin azide complex stretching modes. The Fourier transform infrared layout is shown in Figure 4. The infrared radiation from the source is incident on the beam splitter which divides the beam into two and directs the two beams perpendicularly as shown in Figure 4. The split beams are reflected by moving and stationary mirrors. These reflected beams form constructive and destructive interference patterns based on difference in their path length. These diffraction patterns are generated due to the difference created in the path length of the reflected beam through the motion of the moving mirror. Finally, the recombined beam passes through the sample cell. An intensity versus distance spectrum known as an interferogram is generated. This spectrum is further converted into intensity vs. wave number via Fourier transformation.

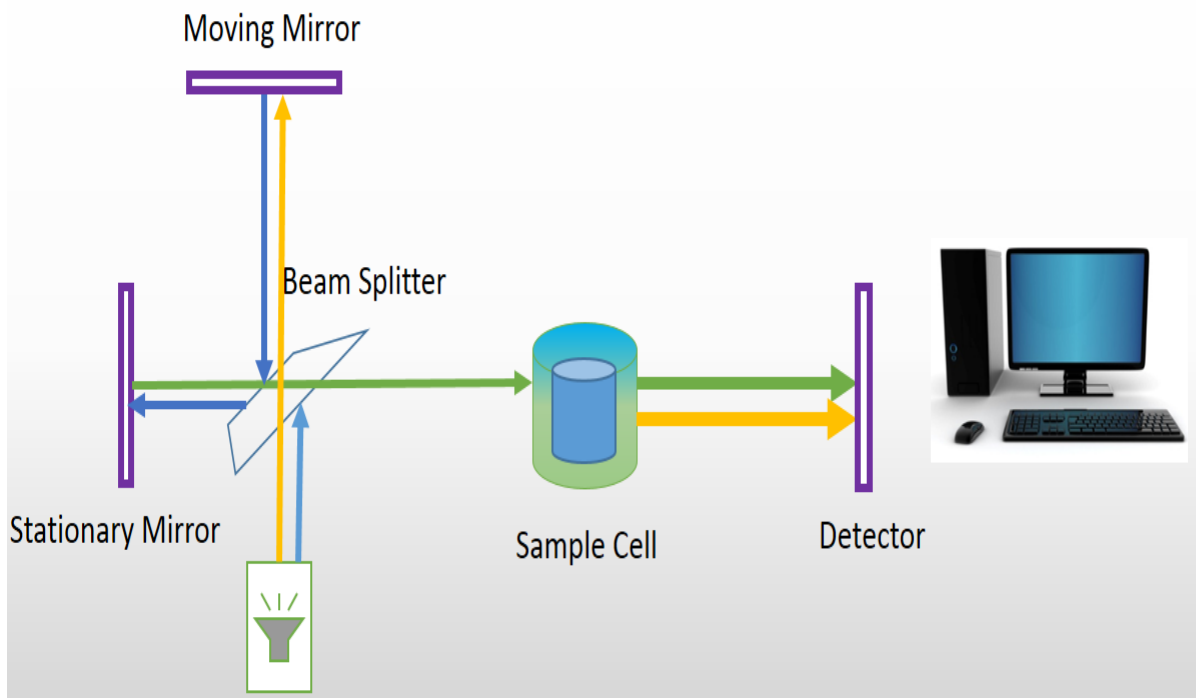


Figure 4 Fourier Transform Infrared Spectrometer

## 2.2 Experiment

All the reagents were purchased from Aldrich and ACROS and used without further purification. KPi buffer stock solutions for each reagent were prepared at 100 mM concentration and pH 7.00. These stock solutions were composed of  $\text{NaN}_3$  and NaF at 1.0 mM and 0.2 M, respectively. DHPA protein was expressed and purified as previously described<sup>43,58</sup>. It was oxidized to the  $\text{Fe}^{3+}$  form by addition of excess potassium ferricyanide ( $\text{K}_4\text{Fe}(\text{CN})_6$ ). The Soret band for ferric heme was observed at a wavelength of 406-407 nm and is known from previous studies to result from a combination of 5-coordinate ferric (60%) and metaquo heme (40%)<sup>34</sup>. The protein concentration was calculated using a molar absorptivity of 116,400  $\text{M}^{-1} \text{cm}^{-1}$  for the Soret band under these conditions.

### 2.2.1 Azide and Fluoride Assays (UV-Vis)

All titrations were carried out in a cuvette with 0.2 cm path length from Starna Cells, Inc. with Agilent 8453 Hewlett Packard Spectrophotometer at 25 °C. The initial volume in the cuvette was 600 µL (DHPA+KPi at pH 7) with the initial protein concentration of 50 µM. A titration of the protein with the respective ligand (azide or fluoride) was conducted by addition of ~ 6-12 µL aliquots of the ligand stock solutions (1.0 mM or 1.5 mM) to the cuvette.

The change in the ligation state of heme was observed by monitoring the shift in the Soret band from 407 to 420 nm in spectra recorded after each aliquot of NaN<sub>3</sub> or NaF<sup>59</sup> was added. These titrations were conducted in the presence of 2,4,6 tri-chlorophenol, 2,4,6 tribromophenol, 2,4 dichlorophenol etc. 7-bromo-indole, 5-bromo-indole, 2,4,6 tri-fluoro phenol, 4-bromophenol.

The concentration of these substrates and inhibitors were maintained 1 mM for each experiment. Once the protein was completely bound with azide ligand the heme spectrum was observed at 420 nm and no shift in the Soret Band was observed if further ~ 6-12 µL aliquots of azide (1.0 mM or 1.5 mM) were added and Normalization of each spectrum was performed depending on the final protein concentration in the cuvette for each titration (reduced because of addition of aliquots of ligands stock solution) and the binding curve was derived based on changes in the spectral region from 300 nm to 700 nm. The analysis was conducted using Igor Pro 7.0. Singular Value Decomposition was performed in Igor for all of the spectra obtained for each titration. Singular value decomposition theorem states that multiplication of three Matrices gives the resultant matrix.  $A_{\text{resultant}} = USV^T$ , where U matrix is the grand mean of

absorbance at wavelength from 300 nm to 700 nm.  $S$  is the difference of each spectrum from the grand mean and  $V^T$  matrix represents the projection of each of those components on individual spectrum.

The apparent binding constants of azide were calculated in presence of different substrates and inhibitors with singular value decomposition and curve fitting analysis.

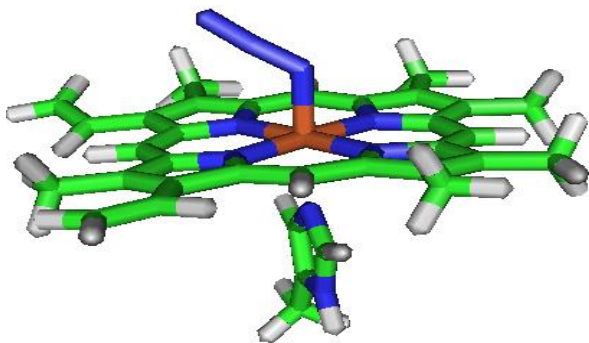


Figure 5 Hemeazide Complex Model

Dehaloperoxidase has at least two internal binding sites<sup>46,60</sup> known from the literature<sup>61</sup>. These two well-established sites are labeled as the  $\alpha$  (substrate) and the  $\beta$  (inhibitor) sites. The  $\beta$ -site was discovered first and shown to be an inhibitor binding site in 2010<sup>29</sup>. The substrate<sup>62</sup> site was observed by X-ray crystallographic structure<sup>34,63</sup> determination<sup>64</sup> and labeled as the  $\alpha$ -site because substrate binding was situated at the  $\alpha$ -edge of the heme<sup>65</sup>. Although the  $\beta$ -site was first observed as an inhibitor binding site, there is evidence from more recent studies that substrates of the peroxygenase function can bind there as well.

Moreover, NMR experiments have shown the different modes of binding in the presence of 2,4,6-TCP and 4-BP<sup>60,66</sup> which strengthens the presence of two different sites in DHP<sup>66</sup>. Previous studies have also shown that different types of substrates such as phenols and

indoles bind in the distal pocket of the protein in one or both of these sites. Moreover, distal pocket<sup>39</sup> is surrounded by the hydrophobic amino acids that stabilizes the internal binding of monohalogenated phenols<sup>67</sup>.

As mentioned the previous studies<sup>59</sup> binding and dissociation of azide with heme follows the same equilibrium model as fluoride.

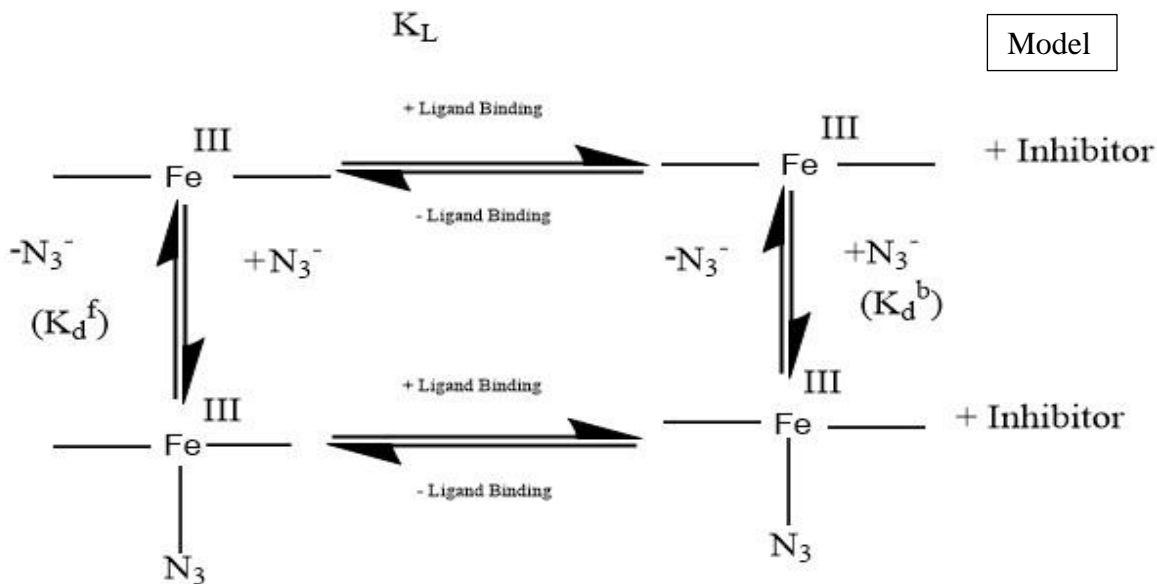


Figure 6 Model for binding of azide to heme

In Figure 6, the model is described the four equilibria between internal ligand-heme-azide, heme-azide and heme-internal ligand.  $K_L$  represents the binding constant for internal binding of inhibitor to heme. Binding constants for Binding of azide to heme and binding of azide to heme-inhibitor are  $K_d^f$  and  $K_d^b$  respectively. From mass conservation law,

$$[E]_0 = [E] + [ES] + [EN_3^-] + [EN_3^-S]$$

$[E]_0$  = Amount of Enzyme Initially Present

$[E]$  = Free Enzyme

[ES] = Enzyme Substrate/Inhibitor

[EN<sub>3</sub>] = Enzyme Azide

[EN<sub>3</sub>S] = Enzyme-azide-substrate/inhibitor

### **2.2.2 Infrared Spectroscopy of Heme Azide Adducts**

Infrared spectra for azide bound DHP were obtained in the presence of various substrates/inhibitors shown in Figure 12. For all experiments, the FX 3000 FTIR Thermo Electron was used and concentration of DHP and azide were 2 mM each. However, the substrates or inhibitor concentrations were 1 mM. Furthermore, baseline correction and curve fitting were completed in Igor Pro 7.0. Analysis gives results shown in Figure 9

FTIR experiments were also performed with varying concentration of DBP (1 mM and 2 mM) with DHP (2 mM) and Azide (2 mM) present. The conditions for the experiments are mentioned in the Figure 9. As shown in Figure 4, the moving mirror speed was maintained as 5KHz or 0.64 cm/sec. Filter is used to improve the signal to noise ratio in FTIR. Resolution of 1 cm<sup>-1</sup> indicates that peaks separated by 1 cm<sup>-1</sup> can be detected from the spectrometer. Sensitivity is the indication of signal to noise ratio which determines whether instrument is of intended use. The numbers of times a interferometer is scanned can be represented by the no of scans in the setting of FTIR. spectrum take in 60 seconds. Beam splitter is an important part of FTIR as it transmits half of the light to fixed mirror and other half to moving mirror. Potassium bromide beam splitter are common in infrared instruments. Infrared radiation source is black carbon for the FTIR. Aperture was left open for the high signal. Changing the aperture size would result in change in the radiation received from a source.

Table 1 FTIR Settings Parameter

Speed	5KHz
Filter	1.2
Resolution	1 cm <sup>-1</sup>
Sensitivity	1
No of Scans	1024
Beam Splitter	KBr
IR Source	SAC1
Beam	Internal
Interferogram Symmetry	Asymmetric
Delay Before Ranging	0
Aperture	Open

### 2.3 Density Functional Theory Calculations

Theoretical comparison of binding strength of ligands in the presence of substrates/inhibitors were performed using density functional theory. Each model was prepared in Materials Studio. The PBE<sup>68</sup> functional and DNP<sup>69</sup> basis set was used for all the calculations in Dmol3.<sup>70,71</sup> A double numerical basis set were used with polarization. The calculations were done on a numerical grid with a cut off of 20 bohrs from each atomic center for the basis set functions. Geometry optimizations were carried out until the convergence criterion was met. Specifically, the change in energy in two subsequent iterations is less of one part in 10<sup>-6</sup> h when convergence is reached. Single point energy calculations were performed

for the optimized structures using COSMO<sup>72</sup> at 0.005 au (1500K) electronic temperature<sup>73</sup>. The dielectric constant was assumed to be 78.4. The PBE functional and DNP basis set were used for all the single point energy calculations as well. To calculate the binding energy of azide, single point energies (SPEs) were calculated for heme-azide, azide and heme complexes. Finally, the SPEs of azide and heme were subtracted from heme-azide complex. This resulting energy is called the azide binding energy. Similar calculations were performed to calculate the binding energy of fluoride.

The barrier for rotation of bound azide in crystal structure was calculated. (Conformation 2) Dihedral angle as shown in the Figure 8 was varied from 0 to 180 degree. A series of single point calculations were performed without optimizing the structures in order to maintain the energies corresponding to original crystal structure. These results are shown in Figure 10 .

## CHAPTER 3

### 3.0 Results

The goal of this study is to develop a method that can be used to determine the binding affinity of substrates and inhibitors that bind in the interior of the DHP globin fold. The competitive binding equilibria between azide and various substrates and inhibitors that bind in the distal pocket will provide information on the relative strength of internal binding.

#### 3.1 Azide Binding Studies

For comparative binding studies with fluoride, the azide binding assay were conducted. These titrations were performed in the presence and absence of substrates and inhibitors. The Soret band was observed at 407 nm in purified DHP isolated using ferricyanide to oxidize the heme to ferric form. Both the X-ray crystal structure and resonance Raman spectroscopy show that the resting state is a mixture of 5cHS or 6cHS (metaquo). The Soret band shifted from 407 to 406 nm as shown in Figure 9, when substrate (e.g. 2,4,6-TCP, 1 mM) or inhibitor (e.g. 4-BP, 1 mM) was added. Addition of aliquots of azide (concentration 0-4 mM) shifted the Soret from 406 nm to 420 nm. In the experiment, Q band changes at 545 nm and 580 nm. Changes in the Q band suggest the existence of six-coordinated heme in the heme azide form. It implies changes in resting state which is mixture of 5cHS or 6cHS (metaquo) to 6cLS which arises when azide is bound as expected based on previous<sup>74</sup> studies.

The dissociation constants for azide in wild type (WT) DHP A and WT DHP B are shown in Table 2. The azide binding affinity for DHPA and DHPB were found to be similar. Their dissociation constants are reported as  $28.7 \pm 4.5 \mu\text{M}$  and  $25.7 \pm 2.8 \mu\text{M}$  respectively.

Table 2 shows that the dissociation constant ( $K_d$ ) for azide is approximately 157 times smaller than the dissociation constant for fluoride in DHPA. The dissociation constants of substrates in the presence of azide and fluoride were not directly obtained. They were correlated with the dissociation constants of ligands. According to our hypothesis, the binding of ligand and substrate is mutually exclusive. It suggests that greater the dissociation constant of ligand in the presence of substrate, greater the binding affinity of substrate. As shown in Table 2, the greatest dissociation constants for azide binding were observed highest in the presence of 2,4-dichlorophenol (2,4-DCP) and 2,4-dibromophenol (2,4-DBP) substrates i.e.  $97.00 \pm 2.03$  and  $227 \pm 1.70$   $\mu\text{M}$ , respectively. Based on these data 2,4-DBP binds 2.3 times more tightly than 2,4-DCP. Similarly, these substrates were found to have the greatest binding affinity in the presence of fluoride. Therefore, irrespective of steric constraints the dihalophenols have greatest binding affinity of all potential DHP substrates.

The binding affinities of azide and fluoride were also observed in the presence of haloindoles. 5-bromoindole has 1.47 and 2 times smaller affinity than 7-bromoindole in the presence of azide and fluoride respectively. It is also noticeable that dissociation constants for azide and fluoride in wild type protein are almost similar unchanged by the binding of the substrate in the presence of 7-bromoindole, resulting in the smallest binding affinity of 7-bromoindole in comparison to other substrates and inhibitors.

The trend for binding affinity of trihalophenols in the presence of azide was observed as  $2,4,6\text{-TCP} > 2,4,6\text{-TBP} > 2,4,6\text{-TFP}$ . Whereas the trend for substrates binding in the presence of fluoride was observed as  $2,4,6\text{-TBP} > 2,4,6\text{-TCP} > 2,4,6\text{-TFP}$ . The different trends in the binding affinities of 2,4,6-TCP and 2,4,6-TBP suggests the presence of steric effect of

azide. It was observed that among all of the trihalophenols. The azide and the fluoride both have the highest binding affinity in the presence of 2,4,6-TFP<sup>75</sup>.

The binding of 2,4,6-TCP is pH dependent. The variation in the pH from 6 to 7 affects drastically the binding affinity of 2,4,6-TCP in the presence of azide. As shown in Table 2, 2,4,6-TCP binds 15.1 times more strongly to heme at pH 6 than at pH 7. Similar trend was observed in the presence of fluoride.<sup>76</sup> Comparison of azide binding to fluoride binding at pH 6 showed that 2,4,6-TCP binds 878 times more than in the presence of fluoride in comparison to the presence of azide.

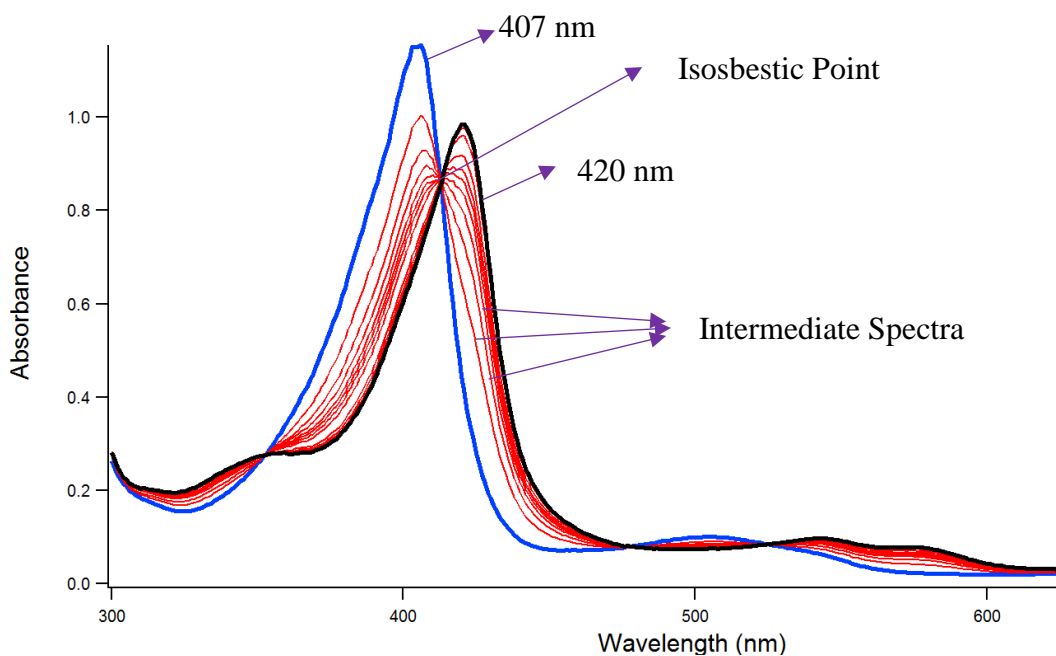


Figure 7 UV-Vis Spectrum of Azide titration of WT DHPA

For indoles, 5-bromoindole has greater binding affinity than 7-bromoindole in the presence of azide. 5-bromoindole binds 379 times more strongly in the presence of fluoride. However, 7-bromoindole binds 280 times less strongly in the presence of azide.

Table 2 Dissociation Constants of azide in WT DHPA & B. Dissociation constants of azide and fluoride in the presence of different substrates and inhibitors in DHPA

<b>Substrates</b>	<b>Azide Binding Constants K<sub>d</sub> (μM)</b>	<b>Fluoride Binding Constants K<sub>d</sub> (mM)</b>	<b>Fluoride/Azide</b>
DHP A WT	28.7 ± 4.5	4.5±0.1	157
DHP B WT	25.7 ± 2.8	4.5±0.4	175
2,4,6 tri-chlorophenol (pH-7)	46.6 ± 3.5	14.5±0.8	311
2,4,6 tri-chlorophenol (pH-6)	666 ± 3.5	38.7 ± 1.4	877
2,4,6 tri-bromophenol	35.7±2.9	23.8±1.0	667
2,4,6 tri-fluorophenol	30.7 ± 3.4	12.7±0.7	413
2,4 dichlorophenol	97.0±2.0	74.1±4.3	764
2,4 dibromophenol	228±1.7	172±9.0	756
7-bromoindole	23.6±3.4	6.6±0.2	280
5-bromoindole	34.8±3.8	13.2±0.5	379
4-bromophenol	27.0 ± 1.6	12.3±0.8	455

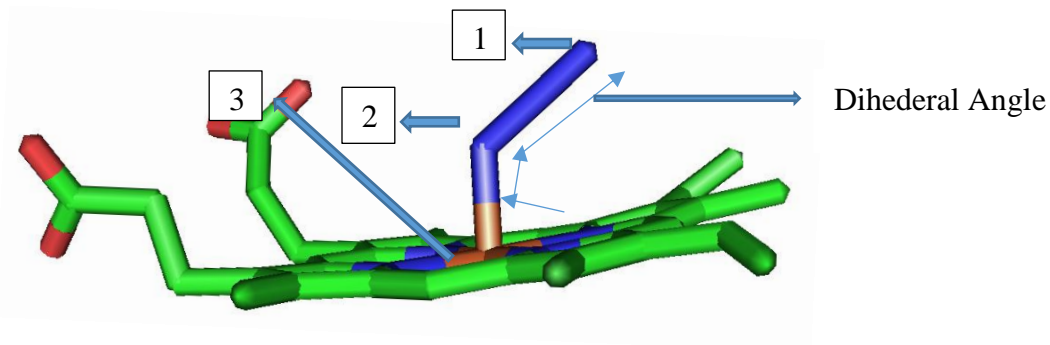


Figure 8 Dihedral Angle ( $\angle 123$ ) for azide rotation

### 3.2 Infrared Spectroscopy

FTIR experiments were performed with azide in the presence of different substrates and inhibitors. Figure S1 shows the two bands were observed for different spin state of iron. The bands at  $2023\text{ cm}^{-1}$  and  $2042\text{ cm}^{-1}$  corresponds to low<sup>54</sup> and high spin of iron, respectively. The intensities of these bands were found to be the function of concentration of 2,4-DBP. As shown in Figure S1: FTIR Spectra of DHP in the presence of different substrates there were also smaller shifts in the bands to higher wavenumber by  $1.0\text{ cm}^{-1}$  for high spin peaks. There was no shift in wavenumber observed in low spin peaks of the spectra.

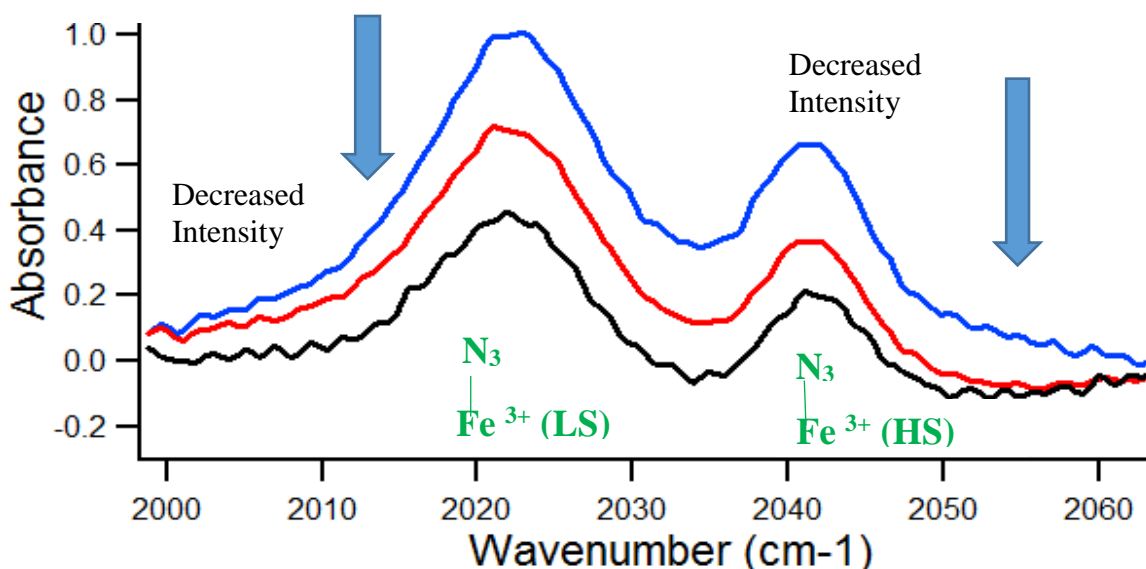


Figure 9 FTIR spectrum a) Blue spectrum: DHP, Azide 2 mM b) Red spectrum: DHP, Azide 2mM and DBP 1 mM c) Black spectrum: DHP, Azide 2mM and DBP 2 mM

### 3.3 Density Functional Theory

Density functional theory calculations were performed to understand more about the internal binding of substrates or inhibitors. Azide binds more tightly than fluoride therefore, from the calculations, the binding affinity of azide and fluoride were reported as 32.6 kcal/mol and 23.4 kcal/mol respectively using Table 3.

Table 3 Single Point Energies of Azide, Fluoride and its adducts in DHP

Complex	Energy (h)	Energy (eV)	Energy (kcal/mol)
Heme	-14.0	-382.7	-8829.3
Azide	-0.6	-17.2	-396.9
Heme-azide complex	-14.7	-401.3	-9258.8
Heme-fluoride complex	-14.4	-391.1	-9018.2
Fluoride	-0.3	-7.2	-165.3

The maximum rotation barrier (Figure 8) was observed when the dihedral angle was changed from 30 to 60 deg and 150 to 180 deg as shown in Figure 10. The highest energy recorded corresponding to rotate the dihedral angle from 30 deg to 60 deg was found to be 7.6 kcal/mol.

Table 4 Binding Energies of azide and Substrate/inhibitor in Dehaloperoxidase

Substrate	Binding Energy of Azide (kcal/mol)	Binding Energy of Substrate/Inhibitor (kcal/mol)
2,4,6-TCP	0	0
2,4,6-TBP	0.7	0.7
4-BP	7.2	7.1
2,4-DCP	0.3	0.2
2,4-DBP	0.7	0.6

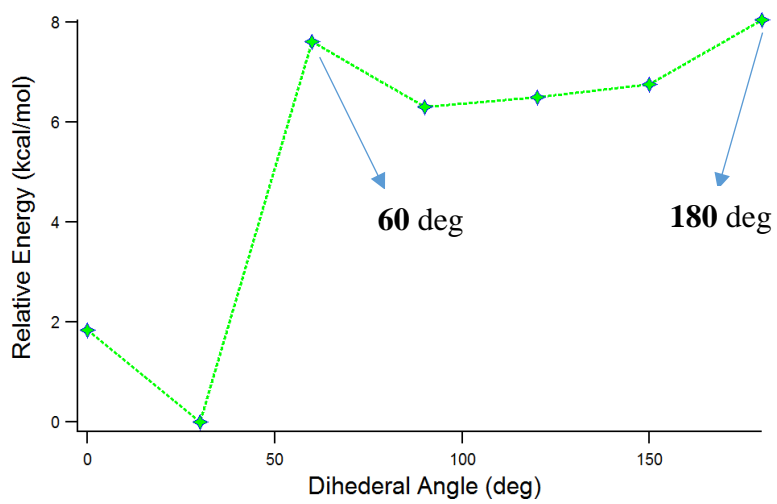


Figure 10 Relative Energy of Rotation

## CHAPTER 4

## 4.0 Discussion

DHP is a multifunctional protein with peroxidase, oxidase, peroxygenase and hemoglobin functions. To develop an understanding of the internal binding mechanism, we have chosen azide for competitive binding studies. Fluoride has already been studied in a competitive binding assay<sup>59</sup>. Therefore, we will compare the fluoride binding data to the azide binding data.

We will understand the data in Table 2 to understand the binding of substrates.

From x-ray crystal structures, we know that there are at least two main binding sites. These are known as  $\alpha$ -site and  $\beta$ -site. The binding site of substrate near the  $\alpha$ -edge is defined as the  $\alpha$ -site. Peroxidase substrate bind at the alpha site at high concentration, therefore, we hypothesize that it can be the peroxygenase binding site. Similarly, the binding site near the  $\beta$ -edge is known as the  $\beta$ -site. Usually, peroxidase inhibitors bind at this site. The inhibitors 4-halphenols bind at the  $\beta$ -site. The 2,4,6 trihalophenols bind at the  $\alpha$ -site and 2,4 dihalphenols appear to bind at both sites,  $\alpha$  and  $\beta$ . The information is so far the best for the mono- and trihalophenols since there are several X-ray crystal structures of each. The information on dihalophenols is of a preliminary nature.

Our goal is to address how substrate binding affects the azide dissociation constants and to relate this information to the structure and function of DHP. To explain this, crystal structures of certain halophenols were overlapped with the azide crystal structure. There is no evidence to suggest that both the substrate and the azide bind simultaneously in DHP. Therefore, our discussion will center on the relative azide dissociation constants as a measure of the binding affinity of substrates in the presence of azide or fluoride. In other words, the binding of azide or fluoride and substrates are mutually exclusive. The crystal structures would

help us comparing the positions of the binding sites of azide and substrates. It will also help us to visualize the steric overlap of the azide and the substrate that might had led to the competitive binding in DHP.

#### 4.1 UV-Vis Spectroscopy

We will systematically compare the phenols starting from 2,4,6 trihalophenols. Figure 12 shows that 2,4,6-TCP has the strongest binding of all the trihalophenols in the presence of azide. There are several factors which account for the different binding affinities of these substrates. First, the distances between (the closest atoms of substrates to heme iron) Fe and chlorine or oxygen of 2,4,6-TCP were found to be 3.8 and 5.0 Å, respectively as shown in b. However, the distance between Fe and bromine of 2,4,6-TBP is 3.6 Å (b). Second, the size of the bromine is bigger than the chlorine. Third, 2,4,6-TBP is pointed towards the binding site of azide (acute angle of binding in comparison to other substrate binding) which create the steric hindrance in the binding of 2,4,6 -TBP if azide is present shown in a. Therefore, 2,4,6-TCP has greater binding affinity than 2,4,6-TBP in the presence of azide. However, converse is true in the presence of fluoride which is smaller in size than azide. It is assumed that 2,4,6-TFP (crystal structure not available) binds right above the heme iron. Also, the smaller size of 2,4,6-TFP lead to the weakest binding affinity in the presence of azide.

Comparison of substrates which bind at  $\beta$ -sites are compared as shown in Figure S4. a) Distance of 2,4,6-TCP and 4-BP closest atom to Fe b) Distance of 2,4,6-TBP and 4-BP closest atom to Fe. Figure 12 represents that in the presence of the azide and the fluoride, 4-BP<sup>77</sup> (PDB 3LB2)<sup>47</sup> binds weakly in comparison to 2,4,6-TCP<sup>64</sup> (PDB 4KMW) and , 2,4,6-TBP<sup>77</sup> (PDB

3ORD). As shown in Figure S4. a) Distance of 2,4,6-TCP and 4-BP closest atom to Fe b) Distance of 2,4,6-TBP and 4-BP closest atom to Fe, the distances between the closest atoms of 4-BP to Fe were found to be 4.1 and 3.6 Å. However, the distances between Fe and the closest chlorine atom to heme iron was measured as 3.8 Å. Also, hydrogen is not shown in the crystal structure resulting relatively more close hydrogen atom of 4-BP to heme than 2,4,6-TCP. Therefore, 4-BP binds closer to the heme iron than 2,4,6-TCP and 2,4,6-TBP. Reasonably, it is displaced easily in the presence of azide or fluoride.

The binding of 2,4,6-TCP varies as the function of pH. At pH 7.5, the 2,4,6-TCP (pKa 6.4) was observed in the phenolate form, therefore, it is unlikely to enter distal pocket<sup>34</sup>. It results in the binding of 2,4,6-TCP at pH 6 binds more than at pH7.

From Table 2, 5-bromindole binds more than 7-bromoindole in the presence of both the azide and the fluoride. We do not understand it completely. The 5-Br-indole binding site is similar to monohalophenol binding site i.e.  $\beta$  site. However, the 7-Br-indole binding site is

similar to the binding site of trihalophenols. This result would explain why 5-Br-indole has greater binding affinity than 7-Br-indole.

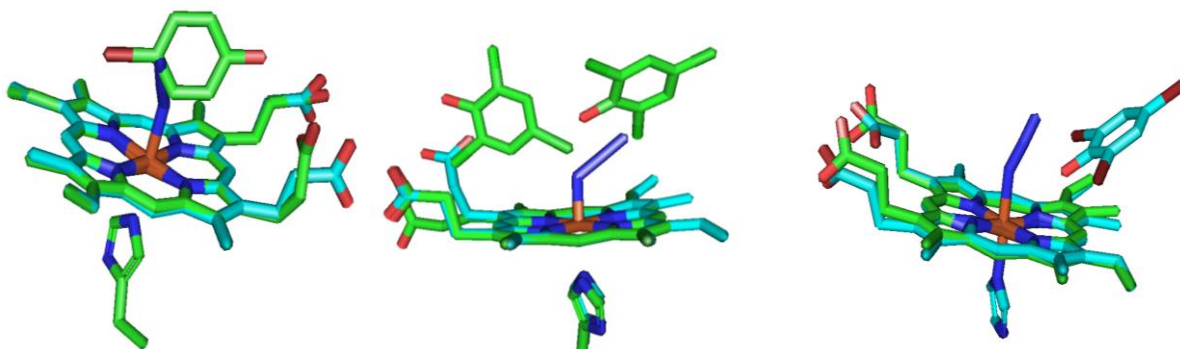


Figure 11 a) Azide (conformation 2) and 4-bromophenol overlapped crystal structures b) Azide (conformation 2) and trichlorophenol overlapped crystal structures c) overlapped crystal structures of azide (conformation 2) and tribromophenol

## 4.2 FTIR

FTIR spectra showed two bands of azide in DHP. These bands at  $2022\text{ cm}^{-1}$  and  $2042\text{ cm}^{-1}$  were found corresponding to low and high<sup>54</sup> spin of iron, respectively. However, in myoglobin low and high spin were observed at  $2023\text{ cm}^{-1}$  and  $2045\text{ cm}^{-1}$ . Therefore, the high spin band differ by three wavenumbers and low spin band differs by one wavenumber between DHP and myoglobin.

Figure S1 shows the spectra in the presence of each substrate. 2,4-DBP shifted the band at  $2042\text{ cm}^{-1}$  shifted by  $1\text{ cm}^{-1}$  which suggests the strongest of 2,4-DBP among all substrates. It was also observed that the intensity of both bands decreased as the function of concentration of 2,4-DBP. The decrease in the intensity of these bands explains that the azide and the 2,4-

DBP cannot bind simultaneously. The binding of 2,4-DBP displaces azide from the distal pocket.

### 4.3 DFT Calculations

As shown in Table 3, DFT calculations showed the azide binds more tightly than fluoride. It agrees with data in Table 2. Computationally, the pattern for azide and fluoride binding affinity was found to be similar what was observed experimentally.

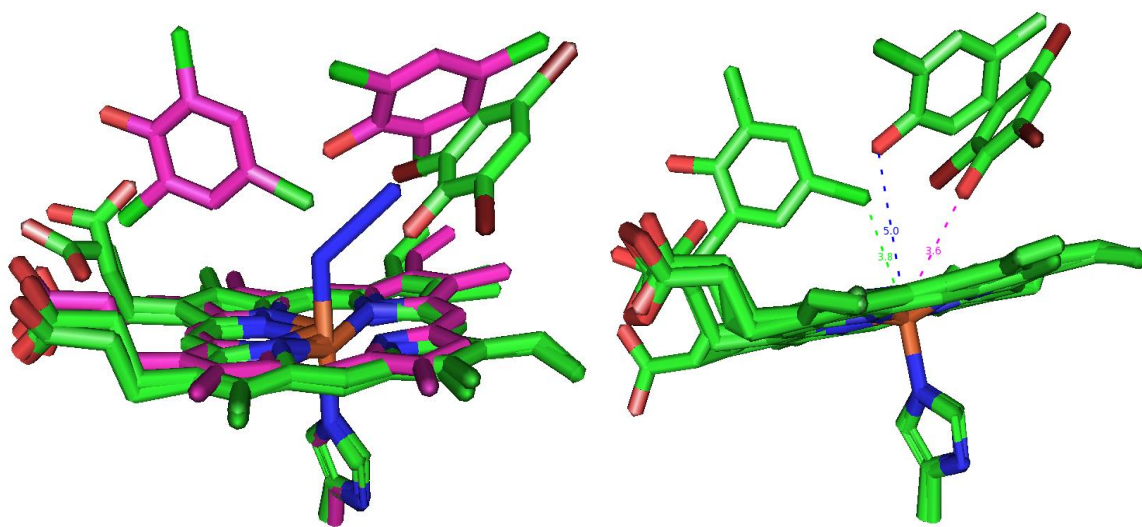


Figure 12 a) Overlapped crystal structures of 2,4,6-TCP, 2,4,6-TBP and Azide (Conformation 2) b) Distances of the closest atoms of 2,4,6-TCP and 2,4,6-TBP from Fe

## CHAPTER 5

## 5.0 Conclusion

To understand the functions of dehaloperoxidase it is necessary to observe the interaction of the substrates with ligands bound to heme. Several ligands like fluoride, cyanide, carbon, azide etc. bind to the ferric form and affect the function of protein. In an earlier study, sodium fluoride binding was studied in a competition assay with various substrates and inhibitors. In this study sodium azide is chosen for comparative studies with fluoride as it is a larger molecule than fluoride. Moreover, the spectroscopic change upon azide binding is also larger since the heme-azide adduct has a low spin heme iron. Thus, the Soret bands shifts from 407 nm in the native ferric complex of DHP, which is a mixture of 5-coordinate HS and the metaquo HS complex, to 420 nm when the LS heme-azide<sup>12</sup> adduct is formed. The other reason for choosing the azide that in spectrochemical series, azide is pi acceptor but fluoride can only contribute to sigma bonding interaction to heme. Apart from these, other factors like Van der Waals forces, hydrogen bonding, electronegativity and smaller flexibility of histidine in the presence of larger ligand (azide) play an important role. From the above discussion and results it was shown that binding affinity of azide/fluoride in the presence of different substrates/inhibitors not only depends on the conformation of bound ligand but also its size, pi-orbitals, Van der Waals interactions, position of substrate/inhibitor, hydrogen bonding etc. Difference in the binding of 2,4,6-TCP and 2,4,6-TBP in the presence of azide/fluoride mostly depends on its steric effect and binding sites of substrates/inhibitors. The difference in the binding affinity of the substrates depends on relative binding and steric effect of the ligands. Azide steric effect was greater for the ligands binding at  $\beta$  site than at  $\alpha$  site binding ligands. 2,4-DBP displaces azide which supports our hypothesis of mutually exclusive binding between the substrates and ligands.

## REFERENCES

1. LaCount, M. W.; Zhang, E.; Chen, Y. P.; Han, K.; Whitton, M. M.; Lincoln, D. E.; Woodin, S. A.; Lebioda, L. The Crystal Structure and Amino Acid Sequence of Dehaloperoxidase from *Amphitrite ornata* Indicate Common Ancestry with Globins. *J. Biol. Chem.* **2000**, *275*, 18712-18716.
2. D'Antonio, E. L.; Bowden, E. F.; Franzen, S. Thin-layer spectroelectrochemistry of the Fe(III)/Fe(II) redox reaction of dehaloperoxidase-hemoglobin. *J. Electroanal. Chem.* **2012**, *668*, 37-43.
3. D'Antonio, E. L.; Chen, T. K.; Turner, A. H.; Santiago-Capeles, L.; Bowden, E. F. Voltammetry of dehaloperoxidase on self-assembled monolayers: Reversible adsorptive immobilization of a globin. *Electrochem. Commun.* **2013**, *26*, 67-70.
4. Du, J.; Huang, X.; Sun, S.; Wang, C.; Lebioda, L.; Dawson, J. *Amphitrite ornata* Dehaloperoxidase (DHP): Investigations of Structural Factors That Influence the Mechanism of Halophenol Dehalogenation Using "Peroxidase-like" Myoglobin Mutants and "Myoglobin-like" DHP Mutants. *Biochem. (N. Y.)* **2011**, *50*, 8172-8180.
5. Weber, R. E.; Mangum, C.; Steinman, H.; Bonaventura, C.; Bonaventura, J.; Sullivan, B. Hemoglobins of two terebellid polychaetes: *Enoplobranchus sanguineus* and *Amphitrite ornata*. *Comp. Biochem. Physiol. A: Physiol.* **1977**, *56*, 179-187.
6. Osborne, R.; Surnithran, S.; Coggins, M.; Chen, Y.; Lincoln, D.; Dawson, J. Spectroscopic characterization of the ferric states of *Amphitrite ornata* dehaloperoxidase and *Notomastus lobatus* chloroperoxidase: His-ligated peroxidases with globin-like proximal and distal properties. *J. Inorg. Biochem.* **2006a**, *100*, 1100-1108.
7. Thompson, M. K.; Davis, M. F.; de Serrano, V.; Nicoletti, F. P.; Howes, B. D.; Smulevich, G.; Franzen, S. Internal Binding of Halogenated Phenols in Dehaloperoxidase-Hemoglobin Inhibits Peroxidase Function. *Biophys. J.* **2010a**, *99*, 1586-1595.
8. Zhao, J.; de Serrano, V.; Zhao, J.; Le, P.; Franzen, S. Structural and Kinetic Study of an Internal Substrate Binding Site in Dehaloperoxidase-Hemoglobin A from *Amphitrite ornata*. *J. Biochem. (N. Y.)* **2013a**, *52*, 2427-2439.
9. Thompson, M.; Franzen, S.; Davis, M.; Oliver, R.; Krueger, J. Dehaloperoxidase-Hemoglobin from *Amphitrite ornata* Is Primarily a Monomer in Solution. *J. Phys. Chem. B* **2011a**, *115*, 4266-4272.

10. De Serrano, V.; D'Antonio, J.; Franzen, S.; Ghiladi, R. A. Structure of dehaloperoxidase B at 1.58 Å resolution and structural characterization of the AB dimer from *Amphitrite ornata*. *Acta Crystallogr., Sect D: Biol. Crystallogr.* **2010**, *66*, 529-538.
11. Han, K.; Woodin, S. A.; Lincoln, D. E.; Fielman, K. T.; Ely, B. *Amphitrite ornata*, a Marine Worm, Contains Two Dehaloperoxidase Genes. *Mar. Biotechnol.* **2001**, *3*, 287-292.
12. D'Antonio, J.; D'Antonio, E.; Thompson, M.; Bowden, E.; Franzen, S.; Smirnova, T.; Ghiladi, R. Spectroscopic and Mechanistic Investigations of Dehaloperoxidase B from *Amphitrite ornata*. *Biochem. (N. Y.)* **2010a**, *49*, 6600-6616.
13. Zhao, J.; Rowe, J.; Franzen, J.; He, C.; Franzen, S. Study of the electrostatic effects of mutations on the surface of dehaloperoxidase-hemoglobin A. *Biochem. Biophys. Res. Commun.* **2012a**, *420*, 733-737.
14. Schkolnik, G.; Utesch, T.; Zhao, J.; Jiang, S.; Thompson, M. K.; Mroginski, M.; Hildebrandt, P.; Franzen, S. Catalytic efficiency of dehaloperoxidase A is controlled by electrostatics – application of the vibrational Stark effect to understand enzyme kinetics. *Biochem. Biophys. Res. Commun.* **2013**, *430*, 1011-1015.
15. Le, P.; Zhao, J.; Franzen, S. Correlation of Heme Binding Affinity and Enzyme Kinetics of Dehaloperoxidase. *Biochem. (N. Y.)* **2014a**, *53*, 6863-6877.
16. Du, J.; Sono, M.; Dawson, J. H. Functional switching of *Amphitrite ornata* dehaloperoxidase from O<sub>2</sub>-binding globin to peroxidase enzyme facilitated by halophenol substrate and H<sub>2</sub>O<sub>2</sub>. *Biochem. (N. Y.)* **2010**, *49*, 6064-6069.
17. Smirnova, T. I.; Weber, R. T.; Davis, M. F.; Franzen, S. Substrate binding triggers a switch in the iron coordination in dehaloperoxidase from *Amphitrite ornata*: HYSORE experiments. *J. Am. Chem. Soc.* **2008**, *130*, 2128.
18. Le, P.; Zhao, J.; Franzen, S. Correlation of Heme Binding Affinity and Enzyme Kinetics of Dehaloperoxidase. *Biochem. (N. Y.)* **2014b**, *53*, 6863-6877.
19. Zhao, J.; Rowe, J.; Franzen, J.; He, C.; Franzen, S. Study of the electrostatic effects of mutations on the surface of dehaloperoxidase-hemoglobin A. *Biochem. Biophys. Res. Commun.* **2012b**, *420*, 733-737.
20. Zhao, J.; de Serrano, V.; Dumariéh, R.; Thompson, M.; Franzen, S. Effect of H55D Mutation on Kinetics and Structure of Dehaloperoxidase-Hemoglobin A. *Biophys. J.* **2011**, *100*, 221a.

21. Nienhaus, K.; Nickel, E.; Davis, M. F.; Franzen, S.; Nienhaus, G. U. Determinants of substrate internalization in the distal pocket of dehaloperoxidase hemoglobin of *Amphitrite ornata*. *Biochem. (N. Y.)* **2008a**, *47*, 12985-12994.
22. Zhao, J.; Lu, C.; Franzen, S. Distinct Enzyme-Substrate Interactions Revealed by Two Dimensional Kinetic Comparison between Dehaloperoxidase-Hemoglobin and Horseradish Peroxidase. *The J. of Phys. Chem..B* **2015a**, *119*, 12828.
23. Franzen, S.; Gilvey, L. B.; Belyea, J. L. The pH dependence of the activity of dehaloperoxidase from *Amphitrite ornata*. *BBA - Proteins and Proteomics* **2007**, *1774*, 121-130.
24. De Serrano, V.; Chen, Z.; Davis, M. F.; Franzen, S. X-ray crystal structural analysis of the binding site in the ferric and oxyferrous forms of the recombinant heme dehaloperoxidase cloned from *Amphitrite ornata*. *Acta Crystallogr., Sect. D: Biol. Crystallogr.* **2007**, *63*, 1094-1101.
25. Zhao, J.; Srajer, V.; Franzen, S. Functional consequences of the open distal pocket of dehaloperoxidase-hemoglobin observed by time-resolved X-ray crystallography. *Biochem. (N. Y.)* **2013b**, *52*, 7943-7950.
26. Barrios, D.; D'Antonio, J.; McCombs, N.; Zhao, J.; Franzen, S.; Schmidt, A.; Sombers, L.; Ghiladi, R. Peroxygenase and Oxidase Activities of Dehaloperoxidase-Hemoglobin from *Amphitrite ornata*. *J. Am. Chem. Soc.* **2014a**, *136*, 7914-7925.
27. Thompson, M. K.; Franzen, S.; Ghiladi, R. A.; Reeder, B. J.; Svistunenko, D. A. Decay of Compound ES in Dehaloperoxidase-Hemoglobin. *Biophys. J.* **2011b**, *100*, 194a-194a.
28. Franzen, S.; Thompson, M. K.; Ghiladi, R. A. The dehaloperoxidase paradox. *BBA - Proteins and Proteomics* **2012**, *1824*, 578-588.
29. Anonymous Protein structure An enzymatic globin from a marine worm. *Nature* **1999**, *401*, 445-445.
30. Belyea, J.; Gilvey, L. B.; Davis, M. F.; Godek, M.; Sit, T. L.; Lommel, S. A.; Franzen, S. Enzyme function of the globin dehaloperoxidase from *Amphitrite ornata* is activated by substrate binding. *Biochem. (N. Y.)* **2005**, *44*, 15637.
31. Feducia, J.; Dumarieh, R.; Gilvey, L.; Smirnova, T.; Franzen, S.; Ghiladi, R. Characterization of Dehaloperoxidase Compound ES and Its Reactivity with Trihalophenols. *Biochem. (N. Y.)* **2009**, *48*, 995-1005.

32. Davydov, R.; Osborne, R. L.; Shanmugam, M.; Du, J.; Dawson, J. H.; Hoffman, B. M. Probing the oxyferrous and catalytically active ferryl states of *Amphitrite ornata* dehaloperoxidase by cryoreduction and EPR/ENDOR spectroscopy. Detection of compound I. *J. Am. Chem. Soc.* **2010**, *132*, 14995-15004.
33. Osborne, R. L.; Coggins, M. K.; Raner, G. M.; Walla, M.; Dawson, J. H. The mechanism of oxidative halophenol dehalogenation by *Amphitrite ornata* dehaloperoxidase is initiated by H<sub>2</sub>O<sub>2</sub> binding and involves two consecutive one-electron steps: role of ferryl intermediates. *Biochem. (N. Y.)* **2009**, *48*, 4231-4238.
34. Thompson, M. K.; Davis, M. F.; de Serrano, V.; Nicoletti, F. P.; Howes, B. D.; Smulevich, G.; Franzen, S. Internal Binding of Halogenated Phenols in Dehaloperoxidase-Hemoglobin Inhibits Peroxidase Function. *Biophys. J.* **2010b**, *99*, 1586-1595.
35. Lu, C.; Lin, Y.; Yeh, S. Inhibitory Substrate Binding Site of Human Indoleamine 2,3-Dioxygenase. *J. Am. Chem. Soc.* **2009**, *131*, 12866-12866.
36. Barrios, D.; D'Antonio, J.; McCombs, N.; Zhao, J.; Franzen, S.; Schmidt, A.; Sombers, L.; Ghiladi, R. Peroxygenase and Oxidase Activities of Dehaloperoxidase-Hemoglobin from *Amphitrite ornata*. *J. Am. Chem. Soc.* **2014b**, *136*, 7914-7925.
37. Cox, R. P.; Hollaway, M. R. The reduction by dithionite of Fe(III) myoglobin derivatives with different ligands attached to the iron atom. A study by rapid-wavelength-scanning stopped-flow spectrophotometry. *Eur. J. Biochem. / FEBS* **1977**, *74*, 575-587.
38. Sun, S.; Sono, M.; Wang, C.; Du, J.; Lebioda, L.; Dawson, J. H. Influence of heme environment structure on dioxygen affinity for the dual function *Amphitrite ornata* hemoglobin/dehaloperoxidase. Insights into the evolutionary structure-function adaptations. *Arch. Biochem. Biophys.* **2014**, *545*, 108-115.
39. Nicoletti, F. P.; Thompson, M. K.; Howes, B. D.; Franzen, S.; Smulevich, G. New insights into the role of distal histidine flexibility in ligand stabilization of dehaloperoxidase-hemoglobin from *Amphitrite ornata*. *Biochem. (N. Y.)* **2010**, *49*, 1903.
40. D'Antonio, J.; Ghiladi, R. A. Reactivity of deoxy- and oxyferrous dehaloperoxidase B from *Amphitrite ornata*: identification of compound II and its ferrous-hydroperoxide precursor. *Biochem.(N. Y.)* **2011**, *50*, 5999-6011.
41. Chen, Z.; De Serrano, V.; Betts, L.; Franzen, S. Distal histidine conformational flexibility in dehaloperoxidase from *Amphitrite ornata*. *Acta Crystallogr., Sect. D: Biol. Crystallogr.* **2009**, *65*, 34-40.

42. Zhao, J.; de Serrano, V.; Franzen, S. A Model for the Flexibility of the Distal Histidine in Dehaloperoxidase-Hemoglobin A Based on X-ray Crystal Structures of the Carbon Monoxide Adduct. *Biochem. (N. Y.)* **2014a**, *53*, 2474-2482.
43. Ma, H.; Thompson, M.; Gaff, J.; Franzen, S. Kinetic Analysis of a Naturally Occurring Bioremediation Enzyme: Dehaloperoxidase-Hemoglobin from Amphitrite ornata. *J. Phys. Chem. B* **2010a**, *114*, 13823-13829.
44. Nicoletti, F. P.; Thompson, M. K.; Franzen, S.; Smulevich, G. Degradation of sulfide by dehaloperoxidase-hemoglobin from Amphitrite ornata. *JBIC J. Biol. Inorg. Chem.* **2011**, *16*, 611-619.
45. D'Antonio, J.; D'Antonio, E. L.; Thompson, M. K.; Bowden, E. F.; Franzen, S.; Smirnova, T.; Ghiladi, R. A. Spectroscopic and mechanistic investigations of dehaloperoxidase B from Amphitrite ornata. *Biochem. (N. Y.)* **2010b**, *49*, 6600-6616.
46. Thompson, M. K.; Davis, M. F.; de Serrano, V.; Nicoletti, F. P.; Howes, B. D.; Smulevich, G.; Franzen, S. Internal Binding of Halogenated Phenols in Dehaloperoxidase-Hemoglobin Inhibits Peroxidase Function. *Biophys. J.* **2010c**, *99*, 1586-1595.
47. Zhao, J.; de Serrano, V.; Franzen, S. A model for the flexibility of the distal histidine in dehaloperoxidase-hemoglobin A based on X-ray crystal structures of the carbon monoxide adduct. *Biochem. (N. Y.)* **2014b**, *53*, 2474-2482.
48. Ma, H.; Thompson, M.; Gaff, J.; Franzen, S. Kinetic Analysis of a Naturally Occurring Bioremediation Enzyme: Dehaloperoxidase-Hemoglobin from Amphitrite ornata. *J. Phys. Chem. B* **2010b**, *114*, 13823-13829.
49. Jing Zhao; Junjie Zhao; Franzen, S. The regulatory implications of hydroquinone for the multifunctional enzyme dehaloperoxidase-hemoglobin from Amphitrite ornata. *J. of Phys. Chem. A* **2013**, *117*, 14615.
50. Szatkowski, L.; Thompson, M. K.; Kaminski, R.; Franzen, S.; Dybala-Defratyka, A. Oxidative dechlorination of halogenated phenols catalyzed by two distinct enzymes: Horseradish peroxidase and dehaloperoxidase. *Arch. Biochem. Biophys.* **2011**, *505*, 22-32.
51. Schechter, A. Hemoglobin research and the origins of molecular medicine. *Blood* **2008**, *112*, 3927-3938.
52. Marengo-Rowe, A. J. Structure-function relations of human hemoglobins. *Proceedings (Baylor University Medical Center)* **2006**, *19*, 239-245.

53. Gulotta, M.; Rogatsky, E.; Callender, R. H.; Dyer, R. B. Primary Folding Dynamics of Sperm Whale Apomyoglobin: Core Formation. *Biophys. J.* **2003**, *84*, 1909-1918.
54. Urayama, P.; Phillips, G. N.; Gruner, S. M. Probing Substates in Sperm Whale Myoglobin Using High-Pressure Crystallography. *Structure* **2002**, *10*, 51-60.
55. Bogumil, R.; Hunter, C.; Maurus, R.; Tang, H.; Lee, H.; Lloyd, E.; Brayer, G.; Smith, M.; Mauk, A. FTIR Analysis of The Interaction of Azide With Horse Heart Myoglobin Variants. *Biochem. (N. Y.)* **1994**, *33*, 7600-7608.
56. Veitch, N. C. Horseradish peroxidase: a modern view of a classic enzyme. *Photochem.* **2004**, *65*, 249-259.
57. Osborne, R.; Raner, G.; Hager, L.; Dawson, J. C-fumago chloroperoxidase is also a dehaloperoxidase: Oxidative dehalogenation of halophenols. *J. Am. Chem. Soc.* **2006b**, *128*, 1036-1037.
58. Zhao, J.; de Serrano, V.; Dumariéh, R.; Thompson, M.; Ghiladi, R.; Franzen, S. The Role of the Distal Histidine in H<sub>2</sub>O<sub>2</sub> Activation and Heme Protection in both Peroxidase and Globin Functions. *J. Phys. Chem. B* **2012c**, *116*, 12065-12077.
59. Alben, J. O.; Fager, L. Y. Infrared studies of azide bound to myoglobin and hemoglobin. Temperature dependence of ionicity. *Biochem. (N. Y.)* **1972**, *11*, 842-847.
60. Zhao, J.; Moretto, J.; Le, P.; Franzen, S. Measurement of internal substrate binding in dehaloperoxidase-hemoglobin by competition with the heme-fluoride binding equilibrium. *The J. of Phys. Chem. B* **2015b**, *119*, 2827-2838.
61. Davis, M.; Gracz, H.; Vendeix, F.; de Serrano, V.; Somasundaram, A.; Decatur, S.; Franzen, S. Different Modes of Binding of Mono-, Di-, and Trihalogenated Phenols to the Hemoglobin Dehaloperoxidase from *Amphitrite ornata*. *Biochem. (N. Y.)* **2009**, *48*, 2164-2172.
62. Zhao, J.; de Serrano, V.; Zhao, J.; Le, P.; Franzen, S. Structural and kinetic study of an internal substrate binding site in dehaloperoxidase-hemoglobin A from *Amphitrite ornata*. *Biochem. (N. Y.)* **2013c**, *52*, 2427.
63. Thompson, M. K.; Davis, M. F.; Franzen, S. Resonance Raman Probes of the Internal Binding Pocket of Dehaloperoxidase from *Amphitrite ornata*. *Biophys. J.* **2009**, *96*, 437a-437a.
64. Michael W. LaCount; Erli Zhang; Yung Pin Chen; Kaiping Han; Margaret M. Whitton; David E. Lincoln; Sarah A. Woodin; Lukasz Lebioda The Crystal Structure and Amino

Acid Sequence of Dehaloperoxidase from *Amphitrite ornata* Indicate Common Ancestry with Globins. *J. Biol. Chem.* **2000**, 275, 18712-18716.

65. Wang, C.; Lovelace, L. L.; Sun, S.; Dawson, J. H.; Lebioda, L. Complexes of dual-function hemoglobin/dehaloperoxidase with substrate 2,4,6-trichlorophenol are inhibitory and indicate binding of halophenol to compound I. *Biochem. (N. Y.)* **2013**, 52, 6203.
66. Zhao, J.; Zhao, J.; Franzen, S. The Regulatory Implications of Hydroquinone for the Multifunctional Enzyme Dehaloperoxidase-Hemoglobin from *Amphitrite ornata*. *J. Phys. Chem. B* **2013d**, 117, 14615-14624.
67. Davis, M.; Bobay, B.; Franzen, S. Determination of Separate Inhibitor and Substrate Binding Sites in the Dehaloperoxidase-Hemoglobin from *Amphitrite ornata*. *Biochem. (N. Y.)* **2010**, 49, 1199-1206.
68. Plummer, A.; Thompson, M. K.; Franzen, S. Role of polarity of the distal pocket in the control of inhibitor binding in dehaloperoxidase-hemoglobin. *Biochem. (N. Y.)* **2013**, 52, 2218.
69. Perdew, J.; Burke, K.; Wang, Y. Generalized gradient approximation for the exchange-correlation hole of a many-electron system. *Phys. Rev. B* **1996**, 54, 16533-16539.
70. Zhang, C.; Shu, Y.; Wang, X.; Zhao, X.; Tan, B.; Peng, R. A new method to evaluate the stability of the covalent compound: by the charges on the common atom or group. *The J. of Phys. Chem. A* **2005**, 109, 6592-6596.
71. Delley, B. From molecules to solids with the DMol(3) approach. *J. Chem. Phys.* **2000**, 113, 7756-7764.
72. Delley, B. An All-Electron Numerical-Method For Solving The Local Density Functional For Polyatomic-Molecules. *J. Chem. Phys.* **1990**, 92, 508-517.
73. Klamt, A.; Schuurmann, G. Cosmo - A New Approach to Dielectric Screening in Solvents With Explicit Expressions For The Screening Energy And Its Gradient. *J. Chem. Soc., Perkin Trans. 2* **1993**, 799-805.
74. Bytheway, I.; Wong, M. W. The prediction of vibrational frequencies of inorganic molecules using density functional theory. *Chem. Phys. Lett.* **1998**, 282, 219-226.
75. Nienhaus, K.; Nickel, E.; Davis, M. F.; Franzen, S.; Nienhaus, G. U. Determinants of substrate internalization in the distal pocket of dehaloperoxidase hemoglobin of *Amphitrite ornata*. *Biochem. (N. Y.)* **2008b**, 47, 12985-12994.

76. Zhao, J.; Moretto, J.; Le, P.; Franzen, S. Measurement of internal substrate binding in dehaloperoxidase-hemoglobin by competition with the heme-fluoride binding equilibrium. *The J. of Phys. Chem. B* **2015c**, *119*, 2827-2838.
77. de Serrano, V.; Franzen, S. Structural evidence for stabilization of inhibitor binding by a protein cavity in the dehaloperoxidase-hemoglobin from *Amphitrite ornata*. *Pept. Sci.* **2012**, *98*, 27-35.
78. Zhao, J.; Franzen, S. Kinetic study of the inhibition mechanism of dehaloperoxidase-hemoglobin a by 4-bromophenol. *The J. of Phys. Chem. B* **2013**, *117*, 8301.

## APPENDIX

## S1. Bands of Azide DHP in the Presence of Substrates/Inhibitors

The shift in the azide band is shown in Figure S1 in the presence of different substrates or inhibitors.

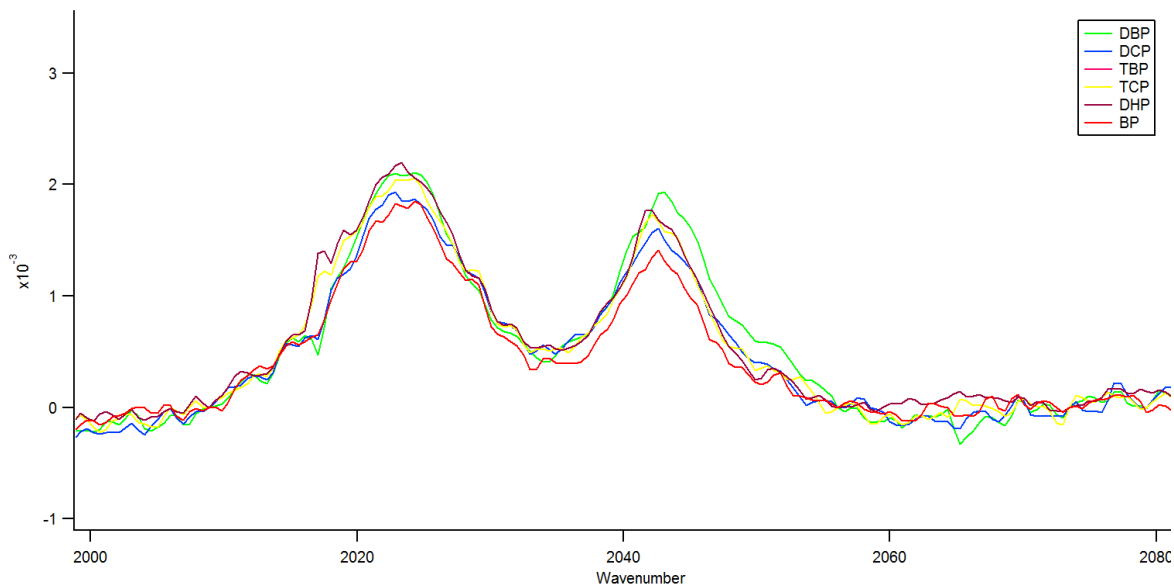


Figure S1: FTIR Spectra of DHP in the presence of different substrates

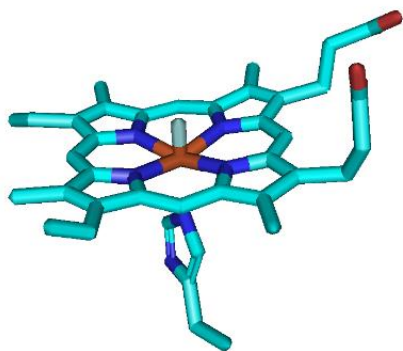


Figure S2: Heme-Fluoride Model

## S2. Overlapped Crystal Structures of Azide And Substrates/Inhibitors

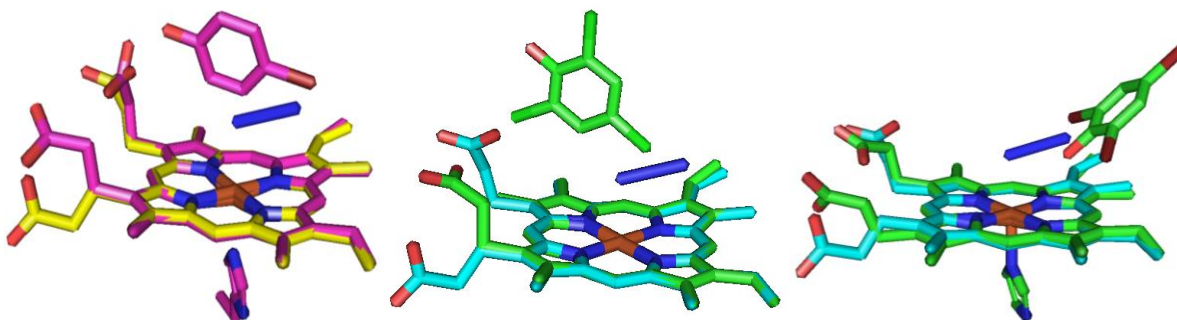


Figure S3. a) Azide (conformation 1) and 4-bromophenol overlapped crystal structures b) Azide (conformation 1) and trichlorophenol overlapped crystal structures c) overlapped crystal structures of azide (conformation 1) and tribromophenol

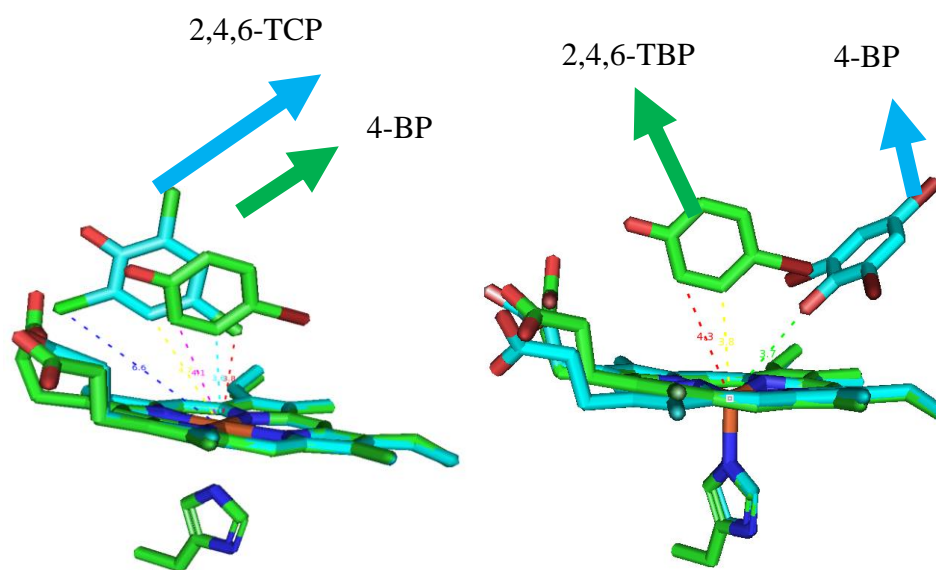


Figure S4. a) Distance of 2,4,6-TCP and 4-BP closest atom to Fe b) Distance of 2,4,6-TBP and 4-BP closest atom to Fe

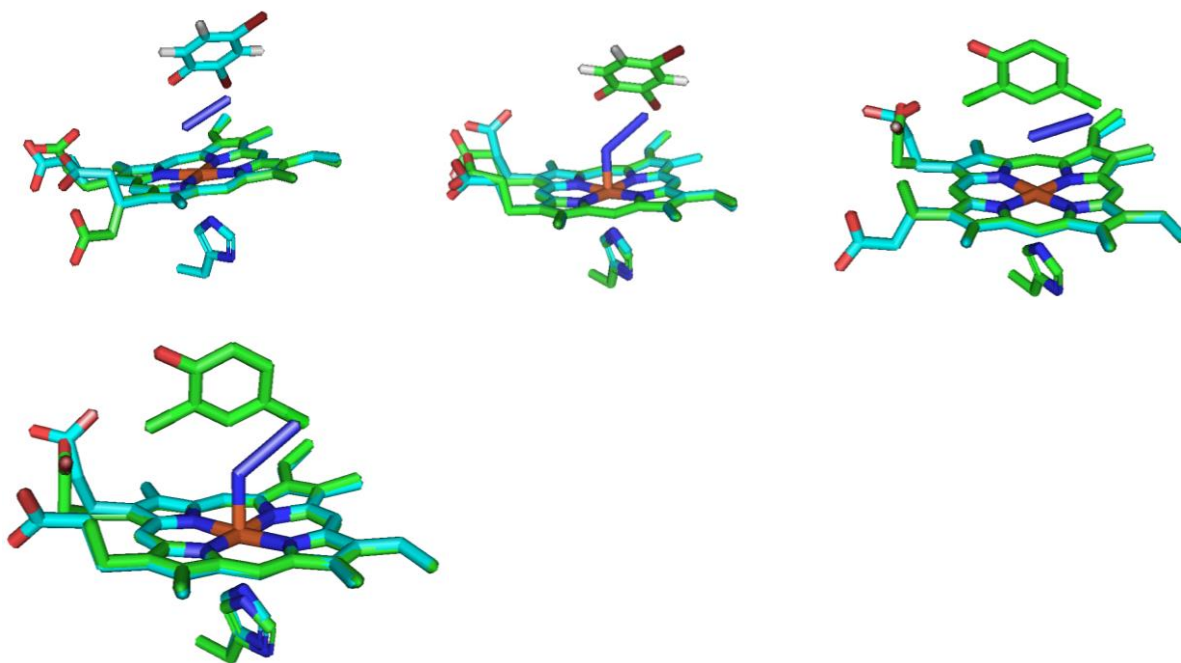


Figure S5. Overlapped Crystal Structures of Azide and Substrates

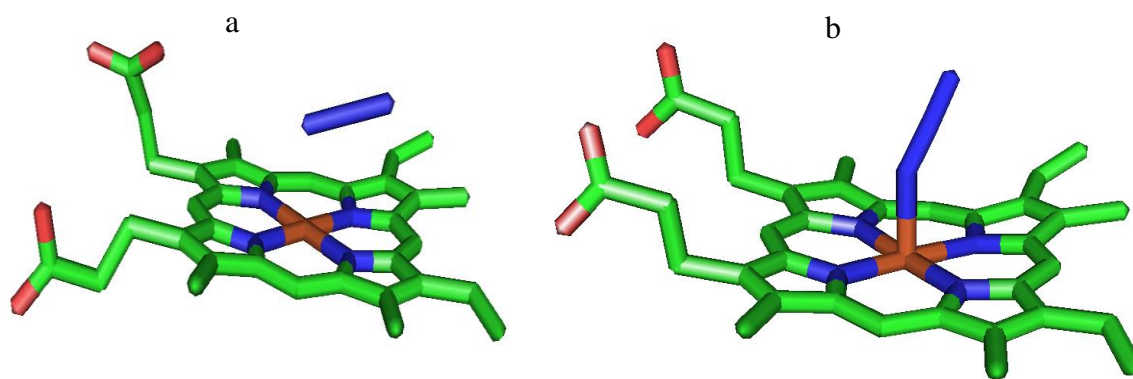


Figure S6. a) Azide Conformation 1 b) Azide Conformation 2